A conserved Bacteroidetes antigen induces anti-inflammatory intestinal T lymphocytes

HHS Public Access

Author manuscript

Science. Author manuscript; available in PMC 2022 December 20.

Published in final edited form as:

Science. 2022 August 05; 377(6606): 660–666. doi:10.1126/science.abg5645.

A conserved Bacteroidetes antigen induces anti-inflammatory intestinal T lymphocytes

Djenet Bousbaine[1,2,3,a], **Laura I. Fisch**[2,†], **Mariya London**[4,†], **Preksha Bhagchandani**[2,3], **Tiago B. R. Castro**[4,5], **Mark Mimee**[3,6,7], **Scott Olesen**[3,8], **Bernardo Reis**[4], **David VanInsberghe**[1,9], **Juliana Bortolatto**[5], **Mathilde Poyet**[3,8], **Ross W. Cheloha**[2], **John Sidney**[10], **Jingjing Ling**[2], **Aaron Gupta**[4], **Timothy K. Lu**[3,6,7], **Alessandro Sette**[10,11], **Eric J. Alm**[3,8], **James J. Moon**[12], **Gabriel D. Victora**[5], **Daniel Mucida**[4,13], **Hidde L. Ploegh**[2,3,*], **Angelina M. Bilate**[3,4,*]

[1]Microbiology Graduate Program, MIT, Cambridge MA, USA.

[2]Program in Cellular and Molecular Medicine, Boston Children's Hospital, Boston MA, USA.

[3]Center for Microbiome Informatics and Therapeutics, MIT, Cambridge MA, USA.

[4]Laboratory of Mucosal Immunology, The Rockefeller University, New York NY, USA.

[5]Laboratory of Lymphocyte Dynamics, The Rockefeller University, New York, NY, USA.

[6]Synthetic Biology Center, MIT, Cambridge MA, USA.

[7]Department of Electrical Engineering and Computer Science, MIT, Cambridge MA, USA.

[8]Department of Biological Engineering, MIT, Cambridge MA, USA.

[9]Department of Civil and Environmental Engineering, MIT, Cambridge MA, USA.

[10]Division of Vaccine Discovery, La Jolla Institute for Immunology, La Jolla CA, USA.

[*]Corresponding authors: Angelina Bilate (abilate@mail.rockefeller.edu) and Hidde Ploegh (Hidde.Ploegh@childrens.harvard.edu).
[a]Present address: Department of Bioengineering, Stanford University, Stanford, CA 94305, USA; Department of Microbiology & Immunology, Stanford University School of Medicine, Stanford, CA 94305, USA; ChEM-H Institute, Stanford University, Stanford, CA 94305, USA.
[†]L. Fisch and M. London contributed equally to this work.

Author contributions: A.M.B., D.B., and H.L.P. conceived the study and wrote the manuscript. A.M.B. and D.B. designed and performed the experiments. D.B. performed the in vitro experiments with help from A.M.B. and P.B.. D.B. and A.M.B. performed the in vivo experiments, with help from L.I.F., M.L., P.B., B.R., and A.G.. T.B.R.C. performed scRNAseq analysis. M.M. and M.P. provided bacterial isolates and M.M. generated all β-hex-deficient strains, under the supervision of T.K.L.. S.O. analyzed the 16S sequencing data under the supervision of E.J.A.. D.V., R.W.C., and J.L. provided support and guidance. J.B. and A.M.B. generated the *Foxp3*-deficient TN mouse line under the supervision of G.D.V.. J.S. performed MHC II peptide binding assays, under the supervision of A.S.. J.J.M. generated tetramers for this study. J.J.M., G.D.V., and D.M. assisted in data interpretation. A.M.B. and H.L.P. supervised the study.

Competing interests: E.J.A. is a consultant and has equities at Finch therapeutics. The other authors declare no competing interests. T.K.L. is a co-founder of Senti Biosciences, Synlogic, Engine Biosciences, Tango Therapeutics, Corvium, BiomX, Eligo Biosciences, Bota.Bio, Avendesora, and NE47Bio. T.K.L. also holds financial interests in nest.bio, Armata, IndieBio, CognitoHealth, Quark Biosciences, Personal Genomics, Thryve, Lexent Bio, MitoLab, Vulcan, Serotiny, Avendesora, Pulmobiotics, Provectus Algae, Invaio, and NSG Biolabs.

Supplementary Materials
Materials and Methods
Figs. S1–S14
Tables S1–S5
Data S1
References (39–55)

[11]Department of Medicine, University of California, San Diego CA, USA.

[12]Center for Immunology and Inflammatory Diseases and Division of Pulmonary and Critical Care Medicine, Massachusetts General Hospital and Harvard Medical School, Boston, MA, USA.

[13]Howard Hughes Medical Institute, The Rockefeller University, New York NY, USA.

Abstract

The microbiome contributes to the development and maturation of the immune system. In response to commensal bacteria, intestinal $CD4^+$ T lymphocytes differentiate into functional subtypes with regulatory or effector functions. The development of small intestine intraepithelial lymphocytes that co-express CD4 and CD8αα homodimers (CD4IELs) depends on the microbiota. However, the identity of the microbial antigens recognized by $CD4^+$ T cells that can differentiate into CD4IELs remains unknown. We identified β-hexosaminidase, a conserved enzyme across commensals of the Bacteroidetes phylum, as a driver of CD4IEL differentiation. In a mouse model of colitis, β-hexosaminidase–specific lymphocytes protected against intestinal inflammation. Thus, T cells of a single specificity can recognize a variety of abundant commensals and elicit a regulatory immune response at the intestinal mucosa.

One-Sentence Summary:

A commensal-derived antigen drives regulatory immune responses in the intestine.

The microbiota contributes to functional specification of adaptive immunity, both through direct interactions and via soluble mediators released into the environment (1–3). Colonic bacteria such as *Helicobacter hepaticus* promote differentiation of antigen-specific $CD4^+$ T cells into $Foxp3^+$ regulatory T cells (Tregs) in the colon, whereas segmented filamentous bacteria (SFB) induce quasi-clonal pro-inflammatory T helper 17 (T_H17) cells in the ileum (4–10). Such interactions are not only specific for the bacterial species concerned, but depending on location and context, can also influence T cell fates (4, 11). Because fate decisions are made at the clonal level, different T cell receptor (TCR) specificities ought to drive distinct developmental and functional outcomes.

Two subsets of $CD4^+$ T lymphocytes are known to regulate adaptive immunity at the intestinal mucosa: peripherally induced regulatory T cells (pTregs) and CD8αα-expressing intraepithelial lymphocytes (CD4IELs) (12–16). Depletion of CD4IELs aggravates intestinal inflammation in mice that lack expression of Foxp3 (14). CD4IELs and pTregs thus cooperate in the regulation of local intestinal inflammation. In specific-pathogen-free (SPF) mice, CD4IELs are present mostly in the small intestinal epithelium (SIE). Their abundance varies with age, diet, and microbiota (17, 18) (fig. S1, A and B and, data S1, A and B). CD4IELs can develop in a microbiota-dependent manner, either from conventional $CD4^+$ T cells or from Treg precursors (11, 14). Germ-free (GF) mice have few if any CD4IELs (14, 19) (fig. S1C). Mice treated with antibiotics show a similar decline in CD4IELs (fig. S1, D and E) (14, 19), whereas fecal transplants from SPF mice restore the CD4IEL population in GF mice to varying extents (fig. S1F) (17, 18). The microbiota therefore contributes not only to the development but also to the maintenance of CD4IELs. However, the microbial antigens recognized by CD4IELs are unknown. Most IEL populations, including

CD4IELs, display a restricted TCR repertoire (17, 20, 21). A limited array of antigens might thus suffice to shape this compartment. We used a microbiota-specific transnuclear (TN) monoclonal T cell model (11) to identify naturally occurring TCR ligands of CD4IELs in SPF mice (fig. S2A). T cells from the TN mouse carry a monoclonal TCR, cloned from a pTreg obtained from a mesenteric lymph node (mLN) of a SPF mouse (11). Naïve monoclonal T cells isolated from TN mice populate not only the recipient's mLNs where they differentiate into pTregs, but also the small intestinal epithelium, where they develop into CD4IELs in a microbiota-dependent fashion (11).

We thus sought to identify the commensal member(s) recognized by TN T cells by selectively growing fecal bacteria derived from Taconic "excluded flora" (EF) mice, which carry a microbiota enriched for the antigen recognized by the TN TCR (11). TN T cells proliferated strongly in the presence of bacterial extracts derived from Bacteroides bile esculin (BBE) agar plates or aerotolerant bacteria recovered from Schaedler blood agar plates (SBA). 16S rRNA sequencing showed enrichment for operational taxonomic units (OTUs) corresponding to the *Parabacteroides* genus in activating extracts (Fig. 1, A to C, and data S1C). TN T cells proliferated robustly in the presence of *Parabacteroides goldsteinii* extracts (Fig. 1D), the predominant member of the altered Schaedler flora (ASF) (22). This proliferation was dependent on antigen presentation by dendritic cells (fig. S2B). Neither the related *Parabacteroides distasonis* nor any other species tested induced proliferation of TN T cells in vitro (Fig. 1D, and fig. S2C). Next, we transferred $CD4^+$ TN T cells into congenic recipients, which were then immunized with bacterial extracts. Proliferation of TN cells occurred in the draining lymph nodes in response to *P. goldsteinii* extract but not *P. distasonis* extract or PBS (Fig. 1E). Thus, *P. goldsteinii*, a commensal abundant in Taconic mice but less so in Jackson (Jax) (fig. S3, A to C, and data S1, D and E), can engage the TN TCR in vivo. TN T cells failed to proliferate and differentiate into CD4IELs in $Rag1^{-/-}$ recipients treated with antibiotics or when colonized with unrelated bacteria (*Clostridium tertium*) but expanded and differentiated into CD4IELs in mice colonized with *P. goldsteinii* (Fig. 1F, and fig. S3D). Thus, *P. goldsteinii* promotes the in vivo development of CD4IELs from naïve T cells carrying the TN TCR.

We next tested whether *P. goldsteinii* could induce CD4IELs in wild-type (WT) mice with a polyclonal T cell repertoire. SPF mice obtained from Jax, which naturally harbor few CD4IELs (fig. S1A), developed more CD4IELs upon colonization with *P. goldsteinii* (Fig. 1G). By contrast, colonization with the unrelated commensal SFB, also absent in Jax mice (10), did not boost CD4IEL frequencies in these mice (fig. S3, E and F). Monocolonization of GF animals with *P. goldsteinii* was not sufficient to induce CD4IELs however (fig. S4A). One possible explanation is that monocolonized mice have low tissue expression of IFNγ and lack class II MHC (MHCII) on intestinal epithelial cells (fig. S4, B to D), both required for CD4IEL development (20, 23). Thus, *P. goldsteinii* promotes the accumulation of CD4IELs from both TN and WT precursors in SPF mice.

We next fractionated *P. goldsteinii* lysates to identify potential TCR ligands derived from this species (fig. S5, A to D). This procedure yielded fractions that activated TN T cells in vitro (fig. S5E). Liquid chromatography with tandem mass spectrometry (LC-MS/MS) analysis of fraction 17 identified 33 proteins, the top 15 of which were expressed

recombinantly in *Escherichia coli* (table S1). Their sonicates served as a source of candidate antigens tested in the proliferation assay. We identified β-*N*-acetylhexosaminidase (β-hex) as the protein recognized by the TN TCR (Fig. 2A). TN T cells proliferated in mice immunized with protein extract of *E. coli* expressing *P. goldsteinii* β-hex, but not when immunized with β-hex derived from closely related species (Fig. 2B). By analyzing the activity of truncated versions of the protein, we defined a ~70-residue stretch that contained the cognate epitope of the TN TCR. Using overlapping peptides, we identified YKGSRVWLN as the minimal epitope (fig. S6, A to D). The corresponding β-hex peptide from *Parabacteroides merdae* failed to stimulate TN T cells, even though it bound to I-A^b (Fig. 2C; fig. S6, E to G; and table S2). Thus, the *P. goldsteinii* YKGSRVWLN β-hex epitope is a natural ligand of the TN TCR. Homologous β-hex peptides derived from *Bacteroides vulgatus* and *Bacteroides luti* also induced proliferation of TN cells in vitro, but only at higher concentrations (Fig. 2D). Using a combination of BlastP and Jackhmmer analyses (24), we found putative β-hex immunostimulatory sequences in many Bacteroidetes members —the most abundant phylum found exclusively in the gastrointestinal tract (25, 26)—as well as in more distantly related species, such as *Spirosoma panaciterrae* (fig. S7). Thus, the TN TCR likely recognizes an even broader collection of bacterial species that belong to the Bacteroidetes phylum.

Colonization of SPF mice with *P. goldsteinii* promoted the expansion and development of CD4IELs and pTregs from TN $CD4^+$ T cells. Likewise, *B. vulgatus*, which also encodes a TN β-hex epitope (Fig. 2D), supported the expansion and development of TN CD4IELs (Fig. 2, E and F, and fig. S8, A to C). By contrast, colonization of mice with a β-hex–deficient strain of *B. vulgatus* failed to do so (fig. S8, D to H). Despite similar expression of β-hex along the intestinal tract (fig. S9, A and B), TN cells transferred into SPF mice proliferated predominantly in the jejunum/ileum–draining mLN (fig. S9, C to E). Thus, the β-hex epitope is presented in the distal mLN and is necessary for the differentiation of CD4IELs from TN precursors.

To determine whether this prevalent β-hex epitope is also recognized by intestinal $CD4^+$ lymphocytes of WT SPF mice, we designed *P. goldsteinii* β-hex–MHCII tetramers spanning the β-hex epitope (table S3) and enumerated β-hex specific $CD4^+$ T cells by flow cytometry (Fig. 3, A to C, and fig. S10, A to L). Splenic $CD4^+$ T cells stained equally poorly with control and β-hex tetramers, whereas β-hex–specific cells were readily identified in both gut-draining mLNs and small intestinal epithelium (Fig. 3, A to C, and fig. S10, A to F). The frequency of β-hex–specific cells was significantly higher among mLNs Tregs of mice housed at both Boston Children's Hospital and Rockefeller University animal facilities (Fig. 3B and S10G). β-hex–specific cells accounted for up to 3.5% of all $CD25^+$ $CD4^+$ T cells (enriched in Tregs (27)) in mLNs (Fig. 3B). Despite the intrinsically reduced ability of CD4IELs to bind MHCII tetramers (fig. S10H), 40% of β-hex $tetramer^+$ cells in the epithelium were CD4IELs (fig. S10, I and J). The frequencies of β-hex–specific $CD4^+$ T cells varied by mouse, with age, and even between rooms within the same facility, and ranged from 1 to 20% in the epithelium and 0.2 to 2% in the mLN (fig. S10, C to F, I, and K). We then examined the extent to which the commensal–derived β-hex antigen shapes the epithelial lymphocyte compartment (Fig. 3C and fig. S10L). In Jax mice, which carry low frequencies of CD4IELs (fig. S1A) and are virtually devoid of *P. goldsteinii* (fig. S3, A and B), the proportion of β-hex–specific IELs was lower than in Taconic

mice (Fig. 3, C and D). Taconic mice have high frequencies of CD4IELs and are natural carriers of intestinal bacteria encoding the β-hex antigen, including *P. goldsteinii* and other Bacteroidetes (See fig. S1E, and fig. S3, A to C). Similarly, Jax mice co-housed with Taconic mice were efficiently colonized with *P. goldsteinii* and showed a higher proportion of β-hex–specific IELs, close to that observed in the Taconic mice themselves (Fig. 3, C and D). Treatment of Jax mice with β-hex peptide slightly increased the frequencies of β-hex–specific IELs, although this difference did not reach statistical significance (Fig. 3C). Thus, the *P. goldsteinii* β-hex epitope is a prominent natural T cell receptor ligand for mLN Tregs and intraepithelial $CD4^+$ T cells. We conclude that a microbiota rich in *P. goldsteinii* supports the expansion of commensal-specific IELs using as example the β-hex antigen derived from abundant intestinal commensals such as *Parabacteroides* and *Bacteroides* spp.

To define the transcriptional signature of β-hex–specific IELs, we index-sorted β-hex^+ and β-hex^- IELs from Taconic mice (fig. S11A), and profiled them by single-cell RNA sequencing (scRNAseq) using the SMART-Seq2 methodology (28). This approach enabled us to analyze the gene expression profile of commensal-induced β-hex–specific IELs at homeostasis. We identified two major clusters visualized by Uniform Manifold Approximation and Projection (UMAP) (Fig. 3E and fig. S11B). Cluster 0 contained mostly *Cd8a* and *Itgae* (encoding CD103)–expressing cells, and a gene signature typical of CD4IELs, which includes both cytotoxic and regulatory profiles as defined by expression of granzymes and *Ctla4* (20, 29). Cluster 1 was composed predominantly of $Cd8a^-$ IELs, including preIELs (20, 29) (fig. S11C). β-hex^+ and β-hex^- IELs were largely indistinguishable from each other and were evenly distributed among the two clusters (Fig. 3E, and fig. S11, D to F). There were no differentially expressed genes between β-hex^+ and β-hex^- IELs, and both subsets expressed typical IEL markers (Fig. 3, F and G, and fig. S11, E to G), associated with both regulatory (i.e., *Ctla4*) and cytotoxic (i.e., *Gzmb*) profiles. We observed a slight enrichment of β-hex^+ IELs in cluster 1 compared to cluster 0 (Fig. 3, F and G, and fig. S11D). This enrichment may be related to the reduced ability of CD4IELs to bind MHCII-tetramers (fig. S10H), presumably because of the inhibitory interactions between the thymus leukemia (TL) antigen on epithelial cells and CD8αα on CD4IELs (30). Thus, the gene expression profile of β-hex–specific IELs is representative of all IELs. Consequently, β-hex likely represents one of many possible specificities that lead $CD4^+$ T cells to acquire an IEL phenotype after initial priming by a commensal antigen.

Although CD4IELs express IFNγ and granzyme B, they display a regulatory phenotype —characterized by the expression of IL-10 and Lag3 (11, 20, 29) (Fig. 3G)—and can protect against intestinal inflammation (14–16). To test the anti-inflammatory potential of β-hex–specific T cells, we transferred $CD4^+$ TN T cells into immunodeficient $Rag2^{-/-}$ mice and then induced colitis by WT $CD4^+$ T cells (fig. S12A) (31). WT cells expanded in the intestine, irrespective of whether TN cells were present or not (fig. S12B). TN cells efficiently differentiated into CD4IELs (fig. S12C). In contrast, they poorly differentiated into pTregs (fig. S12D), similar to what has been observed for other commensal-specific T cells transferred into $Rag1^{-/-}$ recipients (32). TN cells are found predominantly in the small intestine and mLNs (11), but in this colitis model, TN cells were also present in the large intestine, where they acquired expression of CD8αα (fig. S12, B and C). Mice that received TN cells were partially protected from colitis induced by colitogenic WT cells. We observed

reduced weight loss, improved histopathological scores, and lower levels of fecal lipocalin-2 (LCN-2), a marker of intestinal inflammation (33) (Fig. 4, A to D). Oral administration of β-hex peptide—a procedure that expands TN cells and leads to their differentiation into CD4IELs (fig. S12E)—further reduced intestinal inflammation in recipients of TN and WT $CD4^+$ T cells (Fig. 4, B to D). Similarly, mice that received only colitogenic WT cells and oral β-hex peptide also exhibited decreased intestinal inflammation and increased frequency of total CD4IELs in the small intestine (Fig. 4B and fig. S12C). At an earlier time point, we also observed an increased frequency of total CD4IELs as well as of β-hex–specific IELs, which was accompanied by a decreased frequency of Tregs in the epithelium (fig. S12, F to H). The frequency of WT-derived Tregs was low in all groups, suggesting little contribution by pTregs to such protection (fig. S12D), as has been observed previously (34). To definitively exclude a role for WT Tregs, we induced colitis by transferring T cells from *Foxp3*^{DTR} mice and depleted Tregs with diphtheria toxin (DT) (Fig. 4, E to H, and fig. S12, I to J). Depletion of Tregs in this colitis model leads to severe weight loss, intestinal inflammation, and death (35). Despite this depletion, TN T cells still protected mice against intestinal inflammation. Although mice lost weight due to toxicity associated with repeated injections of DT (36, 37), there was no difference between the two groups (recipients of *Foxp3*^{DTR} vs *Foxp3*^{WT} naïve T cells) (Fig. 4, F to H). Similar to WT Tregs, the proportion of TN T cells that differentiated into Tregs was low but not null in this model (fig. S12D). To evaluate a possible contribution of TN-derived Tregs to the anti-inflammatory response induced by β-hex–specific TN T cells, we ablated Foxp3 directly in pTreg TN/*Rag1*$^{-/-}$/*Foxp3*^{eGFP} zygotes using CRISPR/Cas 9 genome editing. We generated mice with either a 1-bp deletion or a 1-bp insertion frameshift in exon 8 of the *Foxp3* gene (fig. S13, A to C). We adoptively transferred splenic $CD4^+$ T cells from these Foxp3-deficient TN mice into *Rag2*$^{-/-}$ recipients and then induced colitis using WT naïve $CD4^+$ T cells as outlined above (fig. S13D). Foxp3-deficient TN T cells (fig. S13E) conferred partial protection against intestinal inflammation (Fig. 4, I to L). Thus, the anti-inflammatory effect exerted by TN T cells in this model can occur in the absence of Foxp3 expression. Notably, Foxp3-deficient and -sufficient TN T cells were equally able to expand in all intestinal sites surveyed (fig. S13F). In this colitis model, TN T cells differentiated into CD4IELs (up to 80%) and secreted IFNγ and granzyme B, which are hallmarks of IELs, irrespective of the presence of a functional *Foxp3* gene in the TN donors (fig. S13, G to I). Thus, β-hex–specific T cells that migrate to, expand within, and differentiate into CD4IELs in response to commensal antigens can protect against intestinal inflammation.

Commensal bacteria shape the differentiation and function of intestinal T cells (1), including CD4IELs. We show that *P. goldsteinii* and other Bacteroidetes can induce antigen-specific differentiation of CD4IELs. It is possible that a fraction of β-hex–specific pTregs generated in the mLNs migrate to the epithelium. There, they can further differentiate into preIELs or CD4IELs after re-encountering their cognate antigen (14, 20). Because $CD4^+$ T cells require local engagement with MHCII to differentiate into CD4IELs (20), recognition of an antigen such as β-hex, present across a range of abundant commensals, may provide CD4IEL precursors with a competitive advantage to populate the intestinal epithelium. Indeed, the same β-hex–specific TCR rearrangement found in the TN strain is present among CD4IELs and their epithelial precursors in mice that carry only the Vβ6 chain of

the TN TCR and a polyclonal TCRα chain (20). Although we have identified β-hex as a natural ligand of intraepithelial $CD4^+$ T cells, it is likely that other commensal-derived antigens are also recognized by these cells. Because activation of CD4IELs is attenuated by interactions between TL antigen expressed by intestinal epithelial cells and CD8αα on IELs (38), antigen abundance and TCR affinity may play a role in the development of CD4IELs. In addition, commensals such as *P. goldsteinii* and *B. vulgatus* may not only provide TCR ligands, but also metabolites essential for the creation of an environment that supports the development and maintenance of regulatory IELs. Here we showed that β-hex–specific T cells that reside in the epithelium can protect against intestinal inflammation. The TCR-titratable regulation imposed by the interaction between the TL antigen and CD8αα (38) may control the anti-inflammatory and cytotoxic functions of CD4IELs. Deciphering the rules that govern the mutualism between commensals, pathobionts, and immune cells is essential for a better understanding of homeostasis and inflammation at the intestinal mucosa.

Supplementary Material

Refer to Web version on PubMed Central for supplementary material.

Acknowledgments:

We thank J. Leube for helping with culture experiments, P. Silver for access to anaerobic chambers, C. McClune for assistance with bioinformatic analyses, S. Jain, J. Bhagat and M. Suarez-Farinas for Statistical consultation, and O. Venezia from the Moon lab for helping with tetramer production. We are grateful to M. Fischbach for supporting D.B. in performing experiments during revision of this manuscript, M. Laub and D. Irvine for guidance throughout the project. We thank S. Kolifrath, A. Rogoz, and S. Gonzalez for mouse husbandry, R. Mathieu from the flow cytometry facilities of BCH and K. Gordon from RU, E. Spooner (WIBR) for mass spectrometry, R. Bronson (Harvard) and Y. Alvarez (RU) and the NYU Histology core facility for histology and colitis scoring, and the NIH tetramer core facility for providing tetramers. We thank members of the Ploegh, Victora, and Mucida laboratories for discussions and suggestions.

Funding:

H.L.P. was supported by CMIT and D.M. by FASI/FARE. D.B. and H.L.P. were supported by NIH R01AI087879 and DP1AI150593-01. A.M.B., M.L., and D.M. by NIH R01DK093674-07, R01DK113375 and R01DK093674. T.B.R.C., J.B. and G.D.V. by NIH DP1AI144248. J.J.M was supported by NIH R01DK126910 and P30DK043351, and MGH ECOR. D.B. is currently funded by an Early Postdoc Mobility Fellowship from the Swiss National Science Foundation.

Data and materials availability:

All data are available in the main text or the supplementary materials. Raw and processed scRNAseq data can be accessed at the Gene Expression Omnibus (GEO) under accession number GSE198037.

References and Notes

1. Belkaid Y, Harrison OJ, Homeostatic Immunity and the Microbiota. Immunity 46, 562–576 (2017). [PubMed: 28423337]
2. Ivanov II, Honda K, Intestinal commensal microbes as immune modulators. Cell Host Microbe 12, 496–508 (2012). [PubMed: 23084918]

3. Geuking MB, Burkhard R, Microbial modulation of intestinal T helper cell responses and implications for disease and therapy. Mucosal Immunology 13, 855–866 (2020). [PubMed: 32792666]
4. Ansaldo E et al. , Akkermansia muciniphila induces intestinal adaptive immune responses during homeostasis. Science 364, 1179–1184 (2019). [PubMed: 31221858]
5. Sefik E et al. , MUCOSAL IMMUNOLOGY. Individual intestinal symbionts induce a distinct population of RORgamma(+) regulatory T cells. Science 349, 993–997 (2015). [PubMed: 26272906]
6. Lathrop SK et al. , Peripheral education of the immune system by colonic commensal microbiota. Nature 478, 250–254 (2011). [PubMed: 21937990]
7. Yang Y et al. , Focused specificity of intestinal TH17 cells towards commensal bacterial antigens. Nature 510, 152–156 (2014). [PubMed: 24739972]
8. Xu M et al. , c-MAF-dependent regulatory T cells mediate immunological tolerance to a gut pathobiont. Nature 554, 373–377 (2018). [PubMed: 29414937]
9. Chai JN et al. , Helicobacter species are potent drivers of colonic T cell responses in homeostasis and inflammation. Sci Immunol 2, eaal5068 (2017). [PubMed: 28733471]
10. Ivanov II et al. , Induction of intestinal Th17 cells by segmented filamentous bacteria. Cell 139, 485–498 (2009). [PubMed: 19836068]
11. Bilate AM et al. , Tissue-specific emergence of regulatory and intraepithelial T cells from a clonal T cell precursor. Sci Immunol 1, eaaf7471 (2016). [PubMed: 28783695]
12. Bilate AM, Lafaille JJ, Induced CD4+Foxp3+ regulatory T cells in immune tolerance. Annu Rev Immunol 30, 733–758 (2012). [PubMed: 22224762]
13. Shale M, Schiering C, Powrie F, CD4(+) T-cell subsets in intestinal inflammation. Immunol Rev 252, 164–182 (2013). [PubMed: 23405904]
14. Sujino T et al. , Tissue adaptation of regulatory and intraepithelial CD4+ T cells controls gut inflammation. Science 352, 1581–1586 (2016). [PubMed: 27256884]
15. Reis BS, Rogoz A, Costa-Pinto FA, Taniuchi I, Mucida D, Mutual expression of the transcription factors Runx3 and ThPOK regulates intestinal CD4(+) T cell immunity. Nat Immunol 14, 271–280 (2013). [PubMed: 23334789]
16. Basu J et al. , Essential role of a ThPOK autoregulatory loop in the maintenance of mature CD4(+) T cell identity and function. Nat Immunol 22, 969–982 (2021). [PubMed: 34312548]
17. Cervantes-Barragan L et al. , Lactobacillus reuteri induces gut intraepithelial CD4(+)CD8alphaalpha(+) T cells. Science 357, 806–810 (2017). [PubMed: 28775213]
18. Umesaki Y, Setoyama H, Matsumoto S, Okada Y, Expansion of alpha beta T-cell receptor-bearing intestinal intraepithelial lymphocytes after microbial colonization in germ-free mice and its independence from thymus. Immunology 79, 32–37 (1993). [PubMed: 8509140]
19. Mucida D et al. , Transcriptional reprogramming of mature CD4(+) helper T cells generates distinct MHC class II-restricted cytotoxic T lymphocytes. Nat Immunol 14, 281–289 (2013). [PubMed: 23334788]
20. Bilate AM et al. , T Cell Receptor Is Required for Differentiation, but Not Maintenance, of Intestinal CD4(+) Intraepithelial Lymphocytes. Immunity 53, 1001–1014 e1020 (2020). [PubMed: 33022229]
21. Wojciech L et al. , Non-canonicaly recruited TCRalphabetaCD8alphaalpha IELs recognize microbial antigens. Sci Rep 8, 10848 (2018). [PubMed: 30022086]
22. Dewhirst FE et al. , Phylogeny of the defined murine microbiota: altered Schaedler flora. Appl Environ Microbiol 65, 3287–3292 (1999). [PubMed: 10427008]
23. Reis BS, Hoytema van Konijnenburg DP, Grivennikov SI, Mucida D, Transcription factor T-bet regulates intraepithelial lymphocyte functional maturation. Immunity 41, 244–256 (2014). [PubMed: 25148025]
24. Eddy SR, Accelerated Profile HMM Searches. PLoS Comput Biol 7, e1002195 (2011). [PubMed: 22039361]
25. Wexler AG, Goodman AL, An insider's perspective: Bacteroides as a window into the microbiome. Nat Microbiol 2, 17026 (2017). [PubMed: 28440278]

26. C. Human Microbiome Project, Structure, function and diversity of the healthy human microbiome. Nature 486, 207–214 (2012). [PubMed: 22699609]
27. Fontenot JD, Gavin MA, Rudensky AY, Foxp3 programs the development and function of CD4+CD25+ regulatory T cells. Nat Immunol 4, 330–336 (2003). [PubMed: 12612578]
28. Trombetta JJ et al. , Preparation of Single-Cell RNA-Seq Libraries for Next Generation Sequencing. Curr Protoc Mol Biol 107, 4 22 21–24 22 17 (2014).
29. London M, Bilate AM, Castro TBR, Sujino T, Mucida D, Stepwise chromatin and transcriptional acquisition of an intraepithelial lymphocyte program. Nat Immunol 22, 449–459 (2021). [PubMed: 33686285]
30. Olivares-Villagomez D et al. , Thymus leukemia antigen controls intraepithelial lymphocyte function and inflammatory bowel disease. Proc Natl Acad Sci U S A 105, 17931–17936 (2008). [PubMed: 19004778]
31. Powrie F, Leach MW, Mauze S, Caddle LB, Coffman RL, Phenotypically distinct subsets of CD4+ T cells induce or protect from chronic intestinal inflammation in C. B-17 scid mice. Int Immunol 5, 1461–1471 (1993). [PubMed: 7903159]
32. Nutsch K et al. , Rapid and Efficient Generation of Regulatory T Cells to Commensal Antigens in the Periphery. Cell Rep 17, 206–220 (2016). [PubMed: 27681432]
33. Chassaing B et al. , Fecal lipocalin 2, a sensitive and broadly dynamic non-invasive biomarker for intestinal inflammation. PLoS One 7, e44328 (2012). [PubMed: 22957064]
34. Izcue A et al. , Interleukin-23 restrains regulatory T cell activity to drive T cell-dependent colitis. Immunity 28, 559–570 (2008). [PubMed: 18400195]
35. Boehm F et al. , Deletion of Foxp3+ regulatory T cells in genetically targeted mice supports development of intestinal inflammation. BMC Gastroenterol 12, 97 (2012). [PubMed: 22849659]
36. Dombrowski Y et al. , Regulatory T cells promote myelin regeneration in the central nervous system. Nat Neurosci 20, 674–680 (2017). [PubMed: 28288125]
37. Goldwich A, Steinkasserer A, Gessner A, Amann K, Impairment of podocyte function by diphtheria toxin--a new reversible proteinuria model in mice. Lab Invest 92, 1674–1685 (2012). [PubMed: 23007132]
38. Olivares-Villagomez D, Van Kaer L, TL and CD8alphaalpha: Enigmatic partners in mucosal immunity. Immunol Lett 134, 1–6 (2010). [PubMed: 20850477]
39. Miura H, Quadros RM, Gurumurthy CB, Ohtsuka M, Easi-CRISPR for creating knock-in and conditional knockout mouse models using long ssDNA donors. Nat Protoc 13, 195–215 (2018). [PubMed: 29266098]
40. Brunkow ME et al. , Disruption of a new forkhead/winged-helix protein, scurfin, results in the fatal lymphoproliferative disorder of the scurfy mouse. Nat Genet 27, 68–73 (2001). [PubMed: 11138001]
41. Rakoff-Nahoum S, Paglino J, Eslami-Varzaneh F, Edberg S, Medzhitov R, Recognition of commensal microflora by toll-like receptors is required for intestinal homeostasis. Cell 118, 229–241 (2004). [PubMed: 15260992]
42. Kino Y et al. , Counterselection employing mutated pheS for markerless genetic deletion in Bacteroides species. Anaerobe 42, 81–88 (2016). [PubMed: 27639596]
43. Mimee M, Tucker AC, Voigt CA, Lu TK, Programming a Human Commensal Bacterium, Bacteroides thetaiotaomicron, to Sense and Respond to Stimuli in the Murine Gut Microbiota. Cell Syst 1, 62–71 (2015). [PubMed: 26918244]
44. Simon MD et al. , Rapid flow-based peptide synthesis. Chembiochem 15, 713–720 (2014). [PubMed: 24616230]
45. Sidney J et al. , Measurement of MHC/peptide interactions by gel filtration or monoclonal antibody capture. Curr Protoc Immunol Chapter 18, Unit 18 13 (2013).
46. Cheng Y, Prusoff WH, Relationship between the inhibition constant (K1) and the concentration of inhibitor which causes 50 per cent inhibition (I50) of an enzymatic reaction. Biochem Pharmacol 22, 3099–3108 (1973). [PubMed: 4202581]
47. Gulukota K, Sidney J, Sette A, DeLisi C, Two complementary methods for predicting peptides binding major histocompatibility complex molecules. J Mol Biol 267, 1258–1267 (1997). [PubMed: 9150410]

48. Valdez Y et al. , Nramp1 drives an accelerated inflammatory response during Salmonella-induced colitis in mice. Cell Microbiol 11, 351–362 (2009). [PubMed: 19016783]

49. Moon JJ et al. , Quantitative impact of thymic selection on Foxp3+ and Foxp3− subsets of self-peptide/MHC class II-specific CD4+ T cells. Proc Natl Acad Sci U S A 108, 14602–14607 (2011). [PubMed: 21873213]

50. Dobin A et al. , STAR: ultrafast universal RNA-seq aligner. Bioinformatics 29, 15–21 (2013). [PubMed: 23104886]

51. Li B, Dewey CN, RSEM: accurate transcript quantification from RNA-Seq data with or without a reference genome. BMC Bioinformatics 12, 323 (2011). [PubMed: 21816040]

52. Stuart T et al. , Comprehensive Integration of Single-Cell Data. Cell 177, 1888–1902 e1821 (2019). [PubMed: 31178118]

53. Maeda H et al. , Quantitative real-time PCR using TaqMan and SYBR Green for Actinobacillus actinomycetemcomitans, Porphyromonas gingivalis, Prevotella intermedia, tetQ gene and total bacteria. FEMS Immunol Med Microbiol 39, 81–86 (2003). [PubMed: 14557000]

54. Gomes-Neto JC et al. , A real-time PCR assay for accurate quantification of the individual members of the Altered Schaedler Flora microbiota in gnotobiotic mice. J Microbiol Methods 135, 52–62 (2017). [PubMed: 28189782]

55. Matsuki T et al. , Development of 16S rRNA-gene-targeted group-specific primers for the detection and identification of predominant bacteria in human feces. Appl Environ Microbiol 68, 5445–5451 (2002). [PubMed: 12406736]

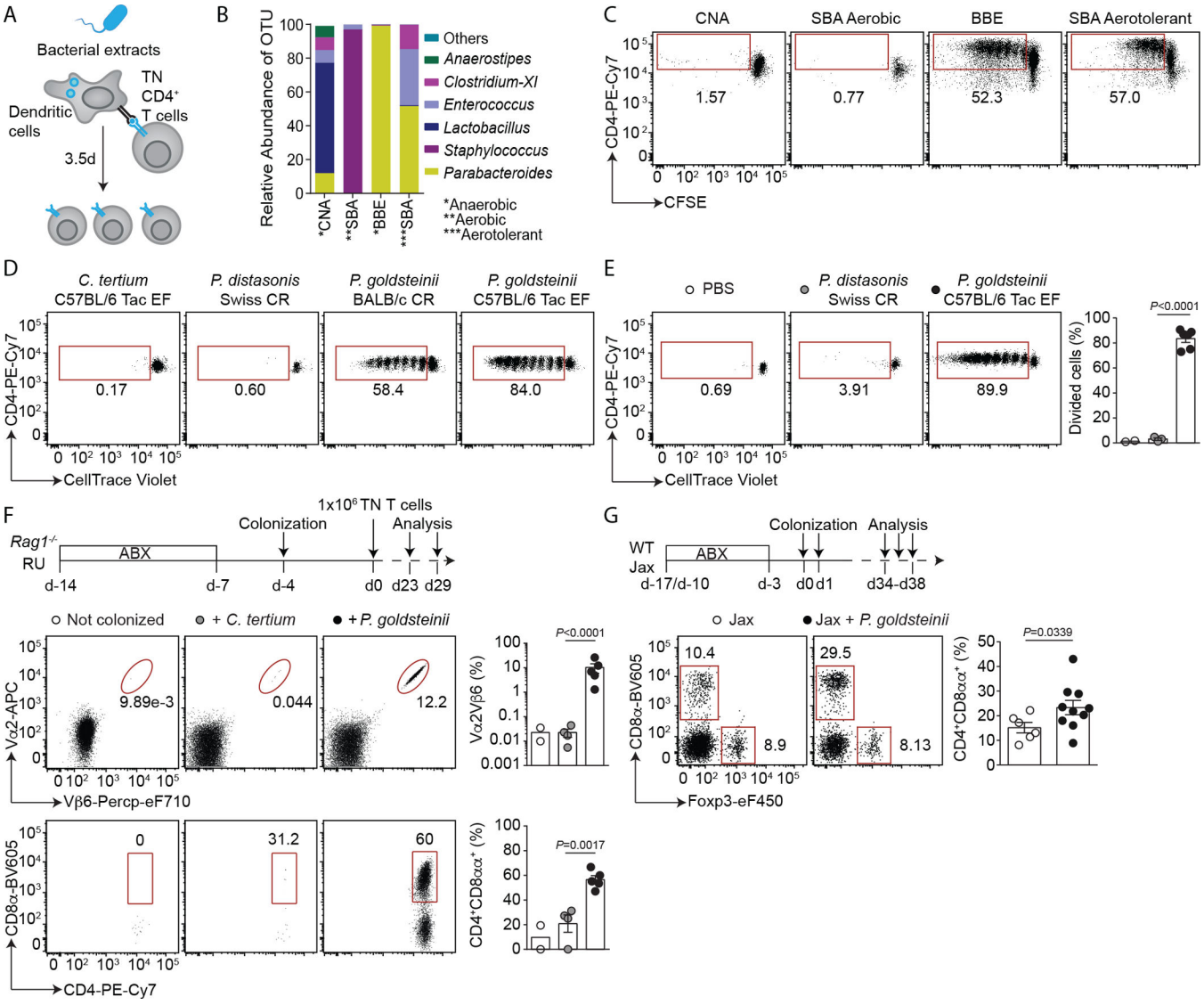

Fig. 1. *P. goldsteinii* induces CD4IELs in both monoclonal and polyclonal SPF mice.

(**A**) Schematic of the in vitro proliferation assay. (**B**) 16S rRNA sequencing of isolated bacterial extracts used in C. (**C**) CFSE dilution among TN cells in response to the indicated bacterial extracts derived from Taconic EF fecal bacteria, isolated using the indicated growth conditions. (**D**) CellTrace Violet dilution among $CD4^+$ TN T cells in response to the indicated bacteria. (C, D) Representative of flow cytometry dot plots of three experiments. (**E**) Representative flow cytometry dot plots showing CellTrace Violet dilution (left) and frequency of divided cells (right) among $CD4^+$ TN T cells harvested from the draining inguinal lymph nodes (LNs) of mice immunized with the indicated bacterial extracts (n=2–6 mice per group). (**F**) *Rag1*$^{-/-}$ hosts were treated with antibiotics (ABX), then either colonized or not colonized with the indicated bacteria prior to receiving $CD4^+$ TN T cells. Cells from the small intestinal epithelium (SIE) were analyzed by flow cytometry (n=2–5). (top) Experimental design. (middle) Representative flow cytometry dot plots of Vα2 and Vβ6 expression among $CD45^+$ cells and CD4 and CD8α expression among TN

cells ($V\alpha2^+V\beta6^+$) in SIE (bottom). (right) Frequency of TN cells among $CD45^+$ cells (top) and frequency of CD4IELs ($CD4^+CD8\alpha\alpha^+$) in the SIE among TN $CD4^+$ T cells (bottom) in all mice analyzed in (F). (**G**) WT Jax mice were treated with ABX and colonized with *P. goldsteinii*. Cells from the SIE were analyzed by flow cytometry (n=6–10). (top) Experimental design. (bottom) Representative dot plots showing Foxp3 and CD8α expression (left) and frequency of CD4IELs (right) among $CD4^+$ T cells. The graphs in (F, G) show the means ± SEM and each symbol represents a mouse from two to three experiments. *P*-values were calculated using unpaired two-tailed Student's *t* test (E and F) and two-tailed Student's *t* test with Welch correction (G). (Tac: Taconic; CR: Charles River; SBA: Schaedler blood agar; BBE: Bacteroides bile esculin; CNA: colistin–nalidixic acid).

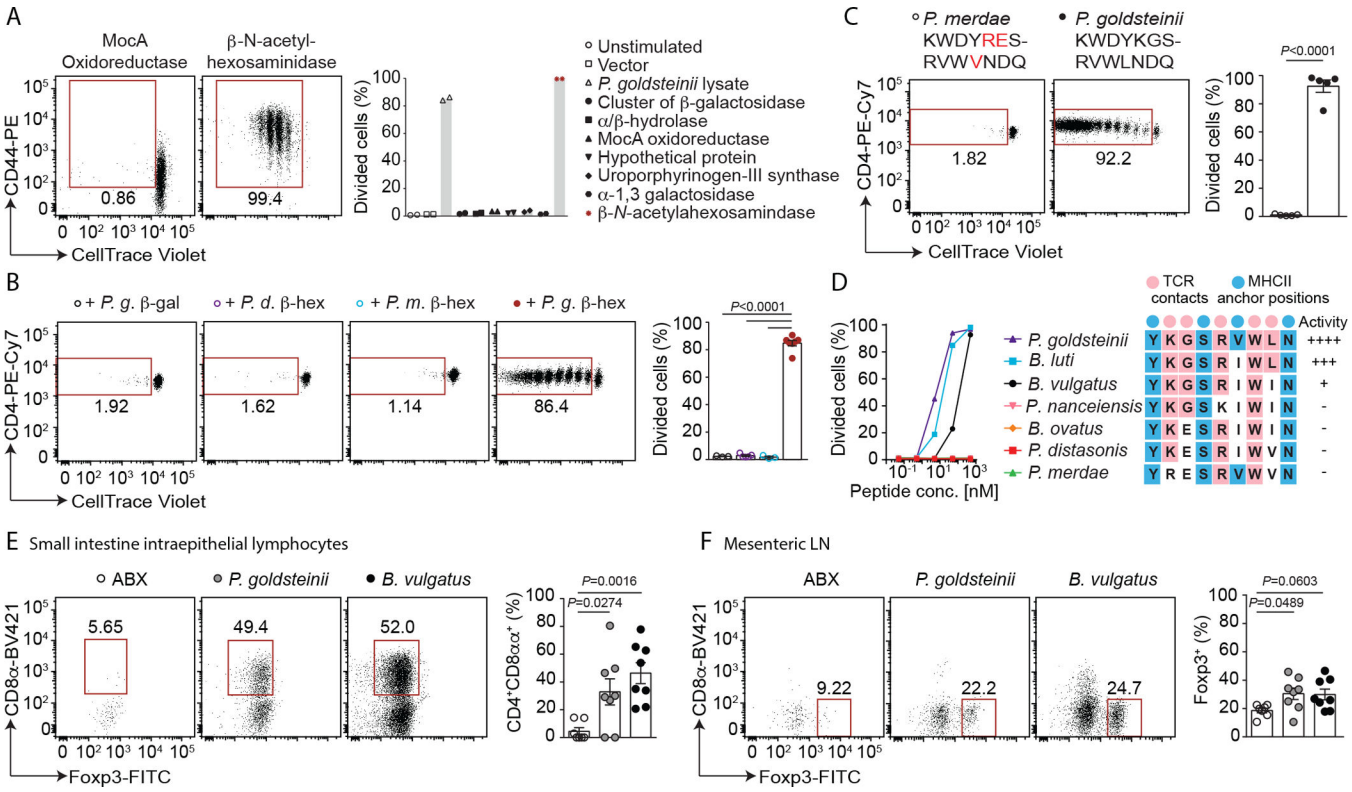

Fig. 2. The TN TCR recognizes epitopes from Bacteroidetes β-*N*-acetylhexosaminidase in complex with I-A^{b}.

(**A**) Candidate polypeptides identified by mass spectrometry were recombinantly expressed in *E. coli* and bacterial extracts were tested in vitro for their ability to activate TN T cells. Representative dot plots (left) and frequency of divided TN T cells in the presence of tested extracts (right). Graph shows means of two technical replicates. (**B** and **C**) In vivo proliferation of CD4^{+} TN T cells in response to 25 μg of bacterial extracts (B, n=3–7) or 2 μg of peptide (C, n=5). Mutations in the core epitope are indicated in red. (**D**) Same as (A), using peptide concentrations of 500 nM-50 pM in serial 10-fold dilutions (left). Alignment of sequences homologous to the TN epitope (right). “Activity” is the ability of each peptide to induce proliferation of TN T cells in vitro (see left). (**E** and **F**) CD45.1^{+} recipients were treated with antibiotics (ABX) and received CD45.2^{+} CD4^{+} TN T cells. The mice were then either colonized or not colonized with the indicated bacteria (n=7–8). Four weeks post-colonization, small intestine intraepithelium lymphocytes (E) and mesenteric lymph nodes (F) were analyzed. Dot plots show CD8α and Foxp3 expression and graphs show the frequency of CD4IELs (CD4^{+}CD8αα^{+}) in the SIE (E) and mLN Tregs (Foxp3^{+}) (F) among TN CD4^{+} T cells. In vitro experiments are representative of three experiments (A and D). Dot plots for in vivo experiments show one representative mouse and the graphs all mice analyzed in two experiments. Each symbol represents a mouse and graphs show means ± SEM (B, C, and E and F). *P*-values were calculated using one-way ANOVA with Dunnett’s post-hoc test in (B, E and F) or unpaired two-tailed Student’s *t* test in (C). (*P.g.*: *P. goldsteinii*; *P.d.*: *P. distasonis*; *P.m.*: *P. merdae*).

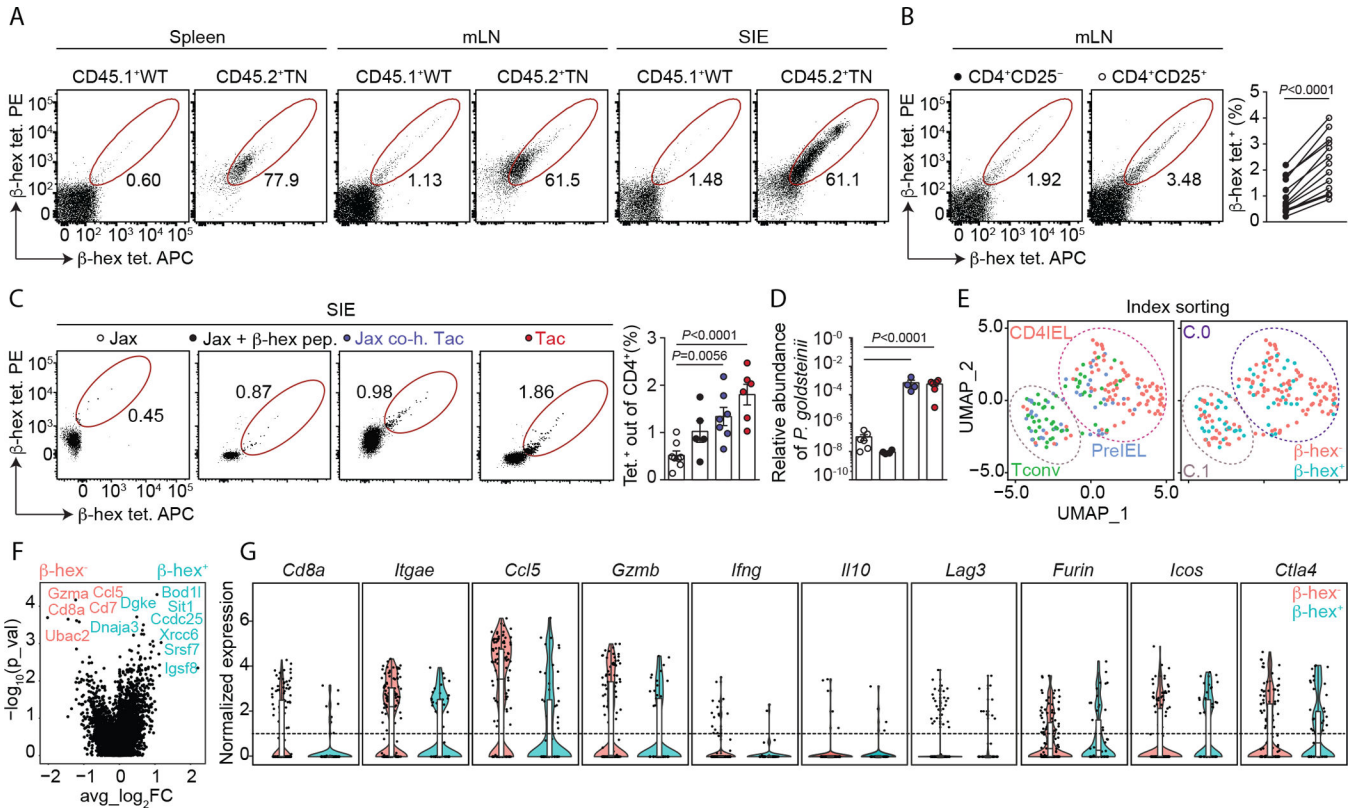

Fig. 3.

The β-hexosaminidase epitope is recognized by intraepithelial lymphocytes and Tregs.

(**A**) Cells from spleen, mesenteric lymph nodes (mLNs), and the small intestinal epithelium (SIE) were harvested from SPF mice housed at BCH. Cells from CD45.1$^+$ WT mice and CD45.2$^+$ TN mice were mixed at 10:1 (WT:TN) ratio and stained with β-hex tetramers. Gates show the frequency of tetramer$^+$ CD45.1$^+$ or CD45.2$^+$ cells among CD4$^+$ T cells. (**B**) Representative dot plots of mLNs from Tac SPF mice (n=13) stained with the indicated tetramers (left). Frequencies of tetramer$^+$ cells in the indicated populations among CD4$^+$ T cells isolated from mLNs (right). (**C**) Tetramer analysis among SIE CD4$^+$ T cells of WT mice sourced from the indicated facilities, co-housed or treated orally with β-hex peptide as indicated (n=5–8 per group). (**D**) Quantification of *P. goldsteinii* abundance by qPCR in fecal samples derived from the mice shown in (C). (**E-G**) scRNAseq analysis of β-hex–specific (β-hex$^+$) and β-hex$^-$ CD4$^+$ T cells sorted from SIE of three Taconic SPF mice. (E) Uniform manifold approximation and projection (UMAP) plots according to gene expression analysis showing the distribution of conventional T cells (Tconv, CD103$^-$ CD8α$^-$), PreIEL (CD103$^+$CD8α$^-$) and CD4IELs (CD103$^+$CD8α$^+$) according to the index sorting (left) and clustering of β-hex$^+$ and β-hex$^-$ cells (right). (F) Volcano plot comparing the gene expression of β-hex$^+$ and β-hex$^-$ cells. (G) Expression of selected genes by β-hex$^+$ and β-hex$^-$ cells. All mice shown of two (E to G), three (A), five (B), or six (C, D) experiments. Error bars represent means ± SEM. *P*-values were calculated using paired two-tailed Student's *t* tests in (B), one-way ANOVA with Dunnett's post-hoc test (C, D) and Wilcoxon rank sum test (F, G). (Jax: Jackson; Tac: Taconic; co-h: co-housed).

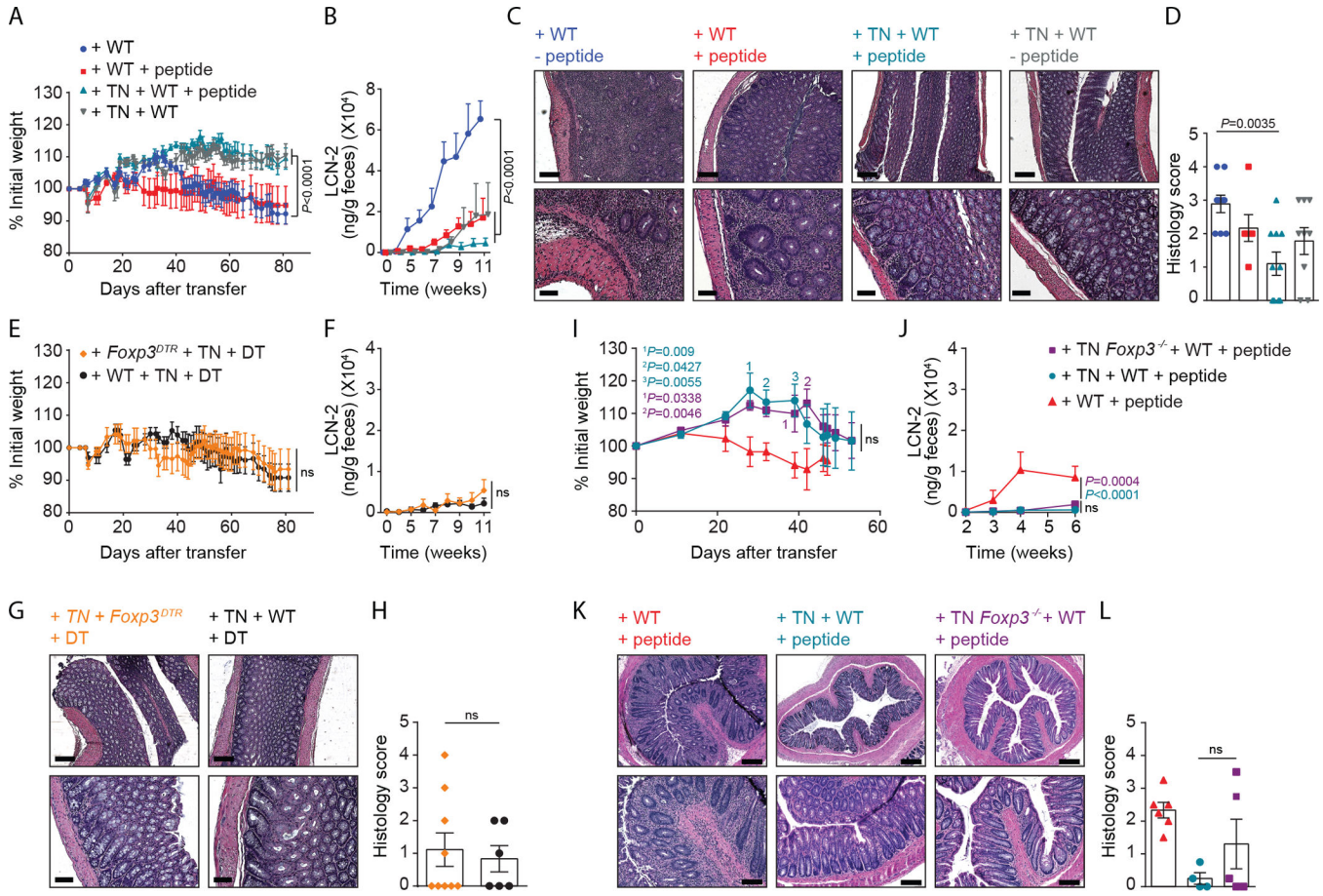

Fig. 4. β-hexosaminidase–specific T cells confer protection against intestinal inflammation.

(**A** to **D**) Taconic SPF *Rag2*$^{-/-}$ either received or did not receive CD45.2^{+}CD4^{+} TN T cells (day 0) and naïve CD45.1^{+} CD4^{+} T cells from WT mice (day 12). On days 2, 4, and 13, some mice received β-hex peptide orally (n=8–10). (A) Percent of initial weight over time. (B) Fecal lipocalin (LCN-2) levels throughout the experiment (n=5–8). (C) Representative photomicrographs of H&E-stained colonic sections from indicated groups. (D) Histology score of H&E-stained sections of colon. (**E** to **H**) Same as (A to D) but using either WT (n=7) or *Foxp3*^{DTR} (n=10) CD4^{+} T cells (on day 12 post-transfer of TN T cells). These mice received diphtheria toxin (DT) intraperitoneally once per week throughout the experiment. (E) Percent of initial weight over time. (F) Fecal LCN-2 levels throughout the experiment. (G) Representative photomicrographs of H&E-stained colonic sections from indicated groups. (H) Histology score of H&E-stained sections of colon. (**I** to **L**) Same as (A to D) but using either WT (n=5) or *Foxp3*$^{-/-}$ TN CD4^{+} cells (n=5, day 0). (I) Percent of initial weight over time. (J) Fecal LCN-2 levels. (K) Representative photomicrographs of H&E-stained sections of colon of indicated groups. (L) Histology scores of H&E-stained sections of colon. (A to L). All mice analyzed in two experiments. Graphs show means ± SEM. *P*-values were calculated using two-way ANOVA for repeated measures with Tukey post-hoc test in (A, B, E, F, I, and J), Mann-Whitney test (H) and Kruskal–Wallis test followed by Dunn's multiple comparisons post-hoc test (D, L). (C and G) Scale bar: 200 μm (top), 60 μm (bottom). (K) Scale bar: 200 μm (top), 100 μm (bottom). Low- and

high-magnification photomicrographs show two representative mice in each group (C and G and K). ns, not significant.